MR angiography of normal intradural vessels of the thoracolumbar spine.

B C Bowen, S DePrima, P M Pattany, A Marcillo, P Madsen and R M Quencer

AJNR Am J Neuroradiol 1996, 17 (3) 483-494
http://www.ajnr.org/content/17/3/483

MR Angiography of Normal Intradural Vessels of the Thoracolumbar Spine

Brian C. Bowen, Steven DePrima, Pradip M. Pattany, Alexander Marcillo, Parley Madsen, and Robert M. Quencer

PURPOSE: To identify and describe the normal intradural vessels detected on MR angiograms of the thoracolumbar spine. **METHODS:** Six adult subjects who had clinical evidence of myelopathy, yet normal findings at spinal digital subtraction angiography (DSA), were also studied without and with contrast-enhanced MR imaging and three-dimensional time-of-flight, single-slab MR angiography. Sagittal and coronal subvolume (targeted) maximum intensity projection images were compared with arterial and venous phase DSA images. Angiographic images were then compared with postmortem, formalin-fixed cord specimens. **RESULTS:** Recognizable intradural vessels were detected only on contrast-enhanced MR angiograms. These vessels corresponded to the posterior and/or anterior median (midline) veins and the great medullary veins. The median veins had variable but mild tortuosity. The medullary veins, which extended from the median veins and coronal venous plexus on the cord surface to the epidural venous plexus, were relatively straight and usually located at T-12 or L-1. The anterior spinal artery could partially contribute to the anterior midline vascular signal. **CONCLUSION:** The intradural vessels identified on contrast-enhanced MR angiograms are primarily veins, and these are usually the largest vessels on or near the cord surface. The limited number and minimal tortuosity of these veins may serve as a baseline for the examination of patients with clinically suspected arteriovenous malformation or fistula.

Index terms: Magnetic resonance angiography; Meninges, magnetic resonance; Spinal cord, anatomy

AJNR Am J Neuroradiol 17:483–494, March 1996

The appearance of spinal vascular malformations on magnetic resonance (MR) angiograms, obtained with the use of either phase-contrast (1–3) or time-of-flight techniques (4), has recently been reported. The authors have suggested that MR angiography may be a useful adjunct to MR imaging in the examination of patients with suspected dural arteriovenous fistulas. In these reports, the vascular malformations were proved by catheter angiography, either conventional (cut-film) or digital subtraction angiography (DSA), and the results were compared with the MR angiographic findings. These studies emphasized the detection of enlarged and tortuous intradural vessels at MR angiography (2–4). Previous investigations of the intradural vascular anatomy in the thoracolumbar region have emphasized the relatively large size of the anterior and posterior median veins on the cord surface, and of the few "great" anterior and/or posterior medullary veins that drain from the cord to the epidural plexus (5–16). The purpose of this article is to describe this appearance in the thoracolumbar region based on a comparison between MR angiograms and catheter angiograms in subjects with normal spinal DSA studies.

Received July 6, 1995; accepted after revision September 25.

From the Departments of Radiology (B.C.B., P.M.P., R.M.Q.) and Neurosurgery (A.M., P.M.), University of Miami School of Medicine, and Doctor's Hospital, Miami, Fla (S.DP.).

Address reprint requests to Brian C. Bowen, PhD, MD, Department of Radiology (R-308), University of Miami School of Medicine, 1115 NW 14th St, Miami, FL 33136.

AJNR 17:483–494, Mar 1996 0195-6108/96/1703–0483

Materials and Methods

Six subjects (age range, 23 to 64 years; mean, 49 years) with various neurologic findings on clinical examination (Table) underwent MR imaging and three-dimensional time-of-flight angiography at 1.5 T, followed by spinal DSA. The length of time between the MR and DSA examinations ranged from 2 days to 6 months. The tech-

Angiographic findings in six subjects with various clinical neurologic findings

Patient	Age, y/Sex	Clinical Findings	Diagnosis	MR Angiography			Digital Subtraction Angiography
				Median Veins*	Medullary Veins	Time Interval	Artery of Adamkiewicz
1	23/M	Diminished sensation to pinprick in saddle area; urinary hesitancy, retention; duration: 1.5 y	Conus medullaris syndrome with myelopathy of unknown origin	T-9 to T-12 (P > A)	R T-12(P) L L-1(P)	6 mo	L T-10
2	57/M	Adult onset diabetes; asymmetric quadriparesis and hyperflexia; duration: 2 y	Cervical spondylitic myelopathy	T-8 to L-1 (P < A)†	R T-12(A) L T-11(P)	2 mo	L T-11
3	40/F	Minimal bilateral LE weakness; intermittent pain, paresthesias L LE; duration: 8 y	Myeloradiculopathy of unknown origin	T-11 to L-1 (P > A)†	R T-10(A) L L-1(P)	7 d	L L-2
4	64/M	Bilateral LE weakness, T-8 sensory level; urinary incontinence; duration: 6 m	HIV-related vacuolar myelopathy (cord biopsy)	T-9 to L-1 (P = A)	R L-1(P)	2 d	L T-12
5	51/M	Bilateral LE weakness and recent numbness; urinary incontinence; duration: 2 m	Chronic inflammatory demyelinating polyneuropathy (conus/cauda equina biopsy)	T-10 to L-1 (P < A)	R T-12(A) L T-12(P)	9 d	R T-11
6	57/F	Lower back pain; R L-5 radiculopathy; R LE weakness; hyperreflexia UE > LE; duration: 9 y	Myelopathy of unknown origin	T-12 to L-1 (P = A)	L T-12(P) R L-1(P)	2 mo	L T-11

Note.—LE indicates lower extremity; UE, upper extremity; P, posterior; A, anterior; and HIV, human immunodeficiency virus.

* Levels over which veins were detected are listed. Visibility of posterior (P) median vein was better than (>), equal to (=), or poorer than (<) that of anterior (A) median vein.

† An anastomosis between anterior and posterior median veins was demonstrated.

niques and conditions for these examinations have been previously described (4). For MR angiography, a single-slab acquisition with coronal or sagittal orientation (approximately parallel to the spinal axis) was positioned so as to encompass the spinal canal. The pulse sequence was a standard radio frequency spoiled gradient-echo sequence (40–50/8–10 [repetition time/echo time], 20° flip angle) with flow compensation along all three coordinate directions. A quadrature spine coil was used, and, with a rectangular field of view, the in-plane resolution was approximately 0.8 mm × 0.9 mm, with section (partition) thickness 0.8 mm. Presaturation bands were positioned to lessen aliasing and motion-induced artifacts. For 3-D slab acquisitions with coronal orientation, bilateral presaturation zones were used. These were each 10 cm wide and encompassed the flanks of the abdomen and lateral chest wall. The medial border of each slab was located approximately one third to one half the distance from the midline to the lateral chest or abdominal wall. For sagittal slab acquisitions, the presaturation zone encompassing the anterior abdomen and chest was 10 cm thick, while the presaturation zone posterior to the spine was approximately 2 to 3 cm, depending on the thickness needed to suppress signal from skin and subcutaneous fat.

MR angiographic data were acquired before and after intravenous administration of a gadolinium chelate. A single precontrast 3-D slab acquisition (sagittal or coronal orientation) and two postcontrast slab acquisitions (sagittal and coronal) were obtained. The postcontrast 3-D acquisitions were begun immediately after bolus infusion (0.2 mmol/kg gadopentetate dimeglumine) and were completed within approximately 20 minutes. The time required to complete an MR examination consisting of the angiographic acquisitions and spin-echo images was approximately 60 minutes.

Postprocessing of the angiographic source images was accomplished with a commercially available, region-of-interest (targeted) maximum intensity projection (MIP) algorithm. MIP images produced from as few as four or five source images were used to locate and display the intradural vessels. MIP images from more source images, or reprojection images, were sometimes necessary to delineate medullary vessels (see "Discussion"). For routine evaluation, a subvolume sagittal angiogram encompassing only 1 to 2 mm on either side of the midline, and a subvolume coronal angiogram encompassing either the posterior or anterior half of the canal were generated.

Spinal cords obtained at autopsy were fixed by immersion in 10% neutral buffered formalin for 2 weeks then transferred to 0.01 mol/L of Sorenson's phosphate buffer for storage at 4°C. The first spinal cord (specimen A) was from a 73-year-old man who died after a heart attack. The second cord (specimen B) was from a 78-year-old man who died after a motor vehicle accident in which the cord

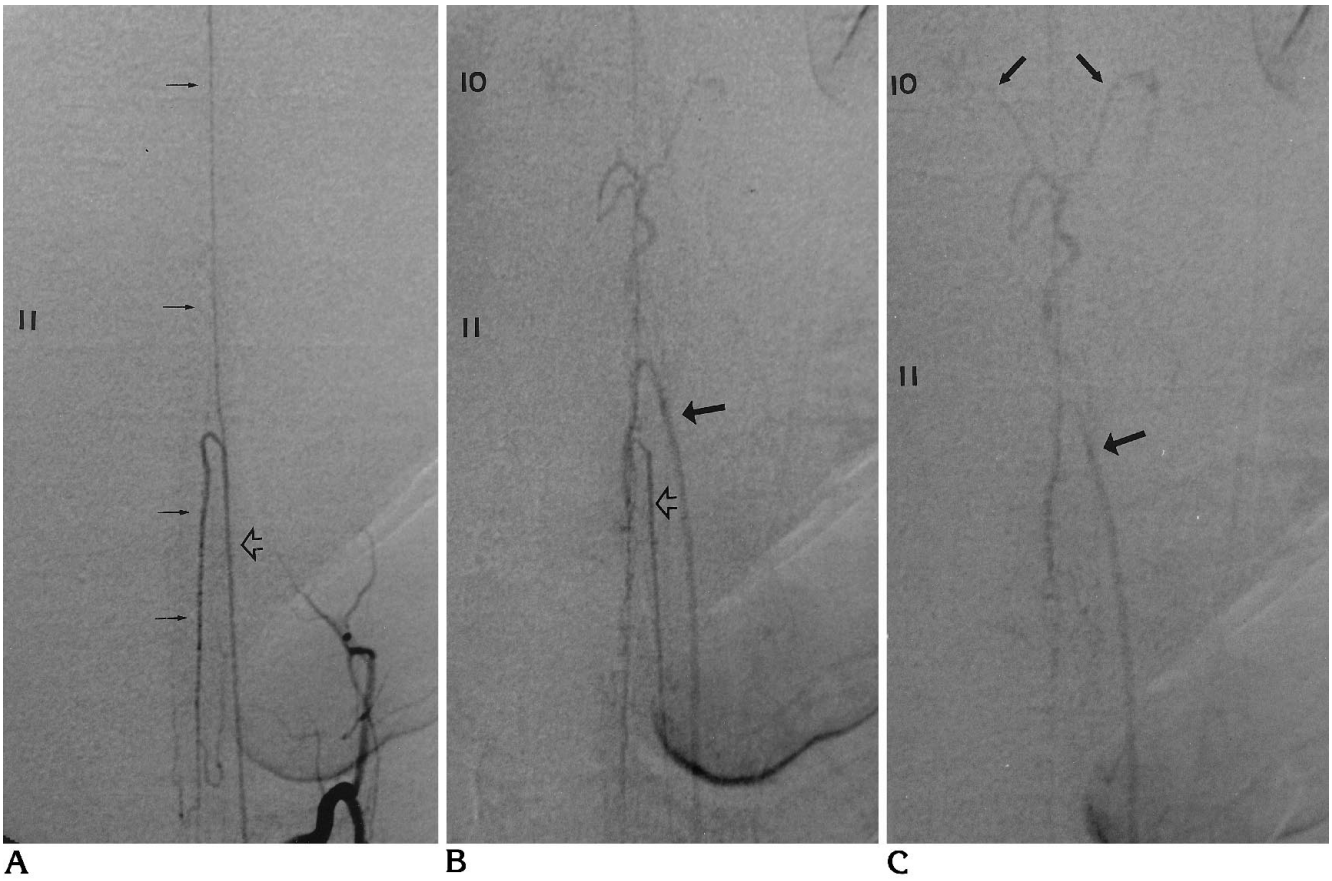

Fig 1. Digital subtraction angiography in subject 3.

A–C, Anteroposterior views 4 seconds (*A*), 13 seconds (*B*), and 20 seconds (*C*) after injection of the left L-2 lumbar artery. In *A*, the great anterior medullary artery (of Adamkiewicz) (*open arrow*) and its ascending and descending branches to the anterior spinal artery (anterior spinal artery, *thin arrows*) are opacified. In *B*, these vessels remain partially opacified owing to a slight prolongation of the injection. The left L-1 great medullary vein (*large arrow*) and midline veins are now seen. The posterior and anterior median veins and the anterior spinal artery are superimposed. In *C*, only the veins are opacified. The veins draining to the left and right T-10 level (*small arrows*) have an atypical ascending course for medullary veins, yet are opacified in the normal temporal sequence. The levels of the neural foramina at the T-10 and T-11 levels are indicated by the numbers *10* and *11* (*Figure continues*).

was not injured. The time from death to autopsy was less than 24 hours in each case.

Results

As illustrated in Figures 1 and 2, DSA showed opacification of the artery of Adamkiewicz, with a characteristic hairpin turn, and the anterior spinal artery within a few seconds after contrast injection. On sequential images, there was a normal temporal sequence of opacification of the anterior spinal artery, posterolateral spinal arteries, posterior and anterior median veins, and draining medullary veins, respectively. Figure 2C and D shows selective injection resulting in opacification of a posterior medullary artery, posterolateral spinal arteries, and, subsequently, intradural veins. Vascular detail on the early (arterial) images was generally better than on the later (venous) images, in part because of patient motion and in part because of dilution of the iodinated contrast material.

The intradural vessels seen on the postcontrast MR angiograms corresponded to the anterior and posterior median veins on the cord surface and to the draining medullary veins seen on the DSA images (compare Figs 1 and 3, and Figs 2 and 4). No vessels corresponding to the posterior medullary arteries or the posterolateral spinal arteries were seen, and, except for possibly a short vascular segment

Figure 1, *continued.*

D, Left anterior oblique view 19 seconds after injection of the left L-2 lumbar artery. The anterior (*small open arrows*) and the larger, more tortuous posterior (*large open arrows*) median veins are shown. The two have an anastomosis (*small arrowhead*) at the T-11 level. The left L-1 medullary vein (*solid arrow*) identified in B is shown to be a posterior draining vein. Note the short kinked segment (*large arrowhead*) of the anterior median vein.

E, Anteroposterior view 3 seconds after injection of the left T-8 intercostal artery. A late venous phase mask has been used for subtraction. The left T-8 anterior medullary artery (*long black arrow*) and the anterior spinal artery (*short black arrows*) are black. The anterior median vein, the right T-10 anterior medullary vein (*white arrows*), and the anastomotic vein at T-11 (*white arrowhead*) are white. The anterior median vein and anterior spinal artery are nearly superimposed at T-10 (indicated by *10*).

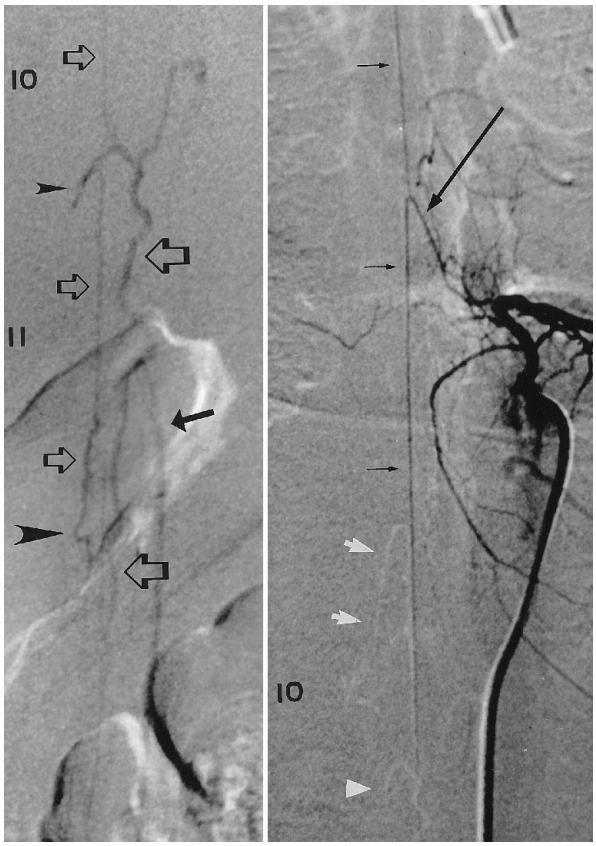

shown in Figure 3B, neither the artery of Adamkiewicz nor the anterior spinal artery was clearly identifiable on the source or MIP images. Precontrast MR angiograms failed to show any of the intradural vessels (Fig 3C). Precontrast MR images in all subjects showed no evidence of cord enlargement. There was no abnormal signal intensity or postcontrast enhancement within the cord except in subject 4, who had diffuse hyperintensity on T2-weighted images between T-9 and T-12, with associated mild enhancement.

Posterior medullary draining veins, delineated on coronal reprojection MR angiograms (Figs 3A and 4A), were identified in all subjects, with the most commonly observed levels being T-12 and L-1. The anterior and posterior medullary veins were not tortuous (Figs 1–4). Sagittal subvolume MIP images (Figs 3D and 4B), produced from source images near the midline, were useful to show the median or paramedian veins that could be correlated with findings on postcontrast T1-weighted spin-echo images (Figs 3E and 4C and D). In four subjects, the posterior median vein was larger than or equal to the anterior median vein (Table 1). The midline vessels were identified over an average distance of four vertebral levels on MR angiograms (3-D acquisition slab length was six to seven levels). The posterior median veins had variable, usually mild, tortuosity, whereas the anterior median vein was relatively straight.

Similar features were noted on the postmortem cord specimens (Fig 5). The anterior median vein was located immediately adjacent and deep to the anterior spinal artery and both had a relatively straight course (Fig 5A). The cephalad and caudad contributions from the median vein to the draining medullary vein were unequal in size, with the caudad segment being larger and of similar size to the medullary vein. These size relationships mimicked those seen for the anterior medullary arteries and their branches to the anterior spinal artery. On both the angiographic studies (Figs 1B and 2C and D) and the postmortem cord specimens, the junction of a medullary vein with a median vein usually had less acute angulation (coathook configuration) than did the junction of a medul-

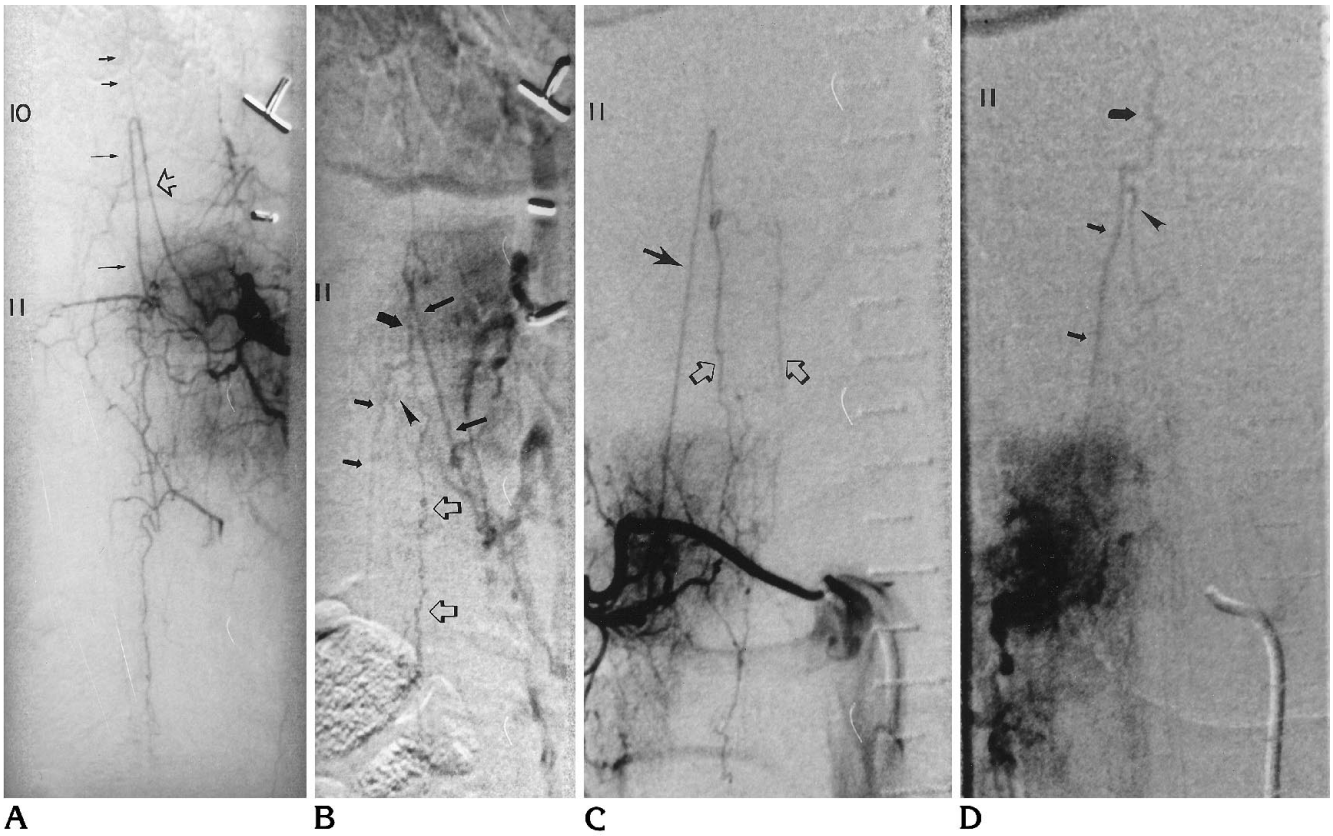

Fig 2. Digital subtraction angiography in subject 6.

A and *B*, Right anterior oblique views 5 seconds (*A*) and 18 seconds (*B*) after injection of the left T-11 posterior intercostal artery. In *A*, the artery of Adamkiewicz (*open arrow*) and its ascending (*short arrows*) and larger descending (*long arrows*) branches to the anterior spinal artery are opacified. In *B*, the right L-1 (*short thin arrows*) and left T-12 (long thin arrows) medullary veins are opacified in a normal temporal sequence. Between their origins, on the cord surface, is a slightly tortuous venous segment (*thick arrow*). Superimposed on this segment is the anterior median vein (*open arrows*), while the posterior median vein (*arrowhead*) is poorly seen. There is a normal T-11 hemivertebral blush.

C and *D*, Anteroposterior views 5 seconds (*C*) and 19 seconds (*D*) after injection of the right L-1 lumbar artery. In C, the right posterior medullary artery (*solid arrow*) and the right and left posterior (or posterolateral) spinal arteries (*open arrows*) are opacified. In D, the right L-1 medullary vein (*thin arrows*), draining from the prominent venous segment (*thick arrow*) on the cord surface, and the posterior median vein (*arrowhead*) are seen better than in B.

lary artery with an anterior or posterolateral spinal artery (hairpin configuration).

Discussion

Vascular Anatomy

The terminology that we use to describe the spinal vascular anatomy delineated by DSA and MR angiography in this study is based primarily on the published works of Gillilan (7, 10), Thron (14), Lasjaunias and Berenstein (15), and Moes and Maillot (11), all of whom expanded upon the pioneering work of Adamkiewicz (17) and Kadyi (18). This terminology is discussed in the following sections.

Arteries.—Each thoracolumbar vertebral segment is largely supplied by dorsal rami, dorsospinal arteries (15), originating from paired segmental arteries (ie, posterior intercostal or lumbar arteries). The intraspinal, or spinal, branch of the dorsal ramus enters the neural foramen, gives off small epidural arteries, and becomes the meningoradicular artery (15), or the radicular-medullary-dural artery (19) (Fig 6). The dural branches originate proximally, and the remaining radicular-medullary artery (19) is often simply referred to as the spinal "radicular artery" (5, 13, 14, 15). The designation *radicular-medullary artery* is preferable because it implies that both radicular and medul-

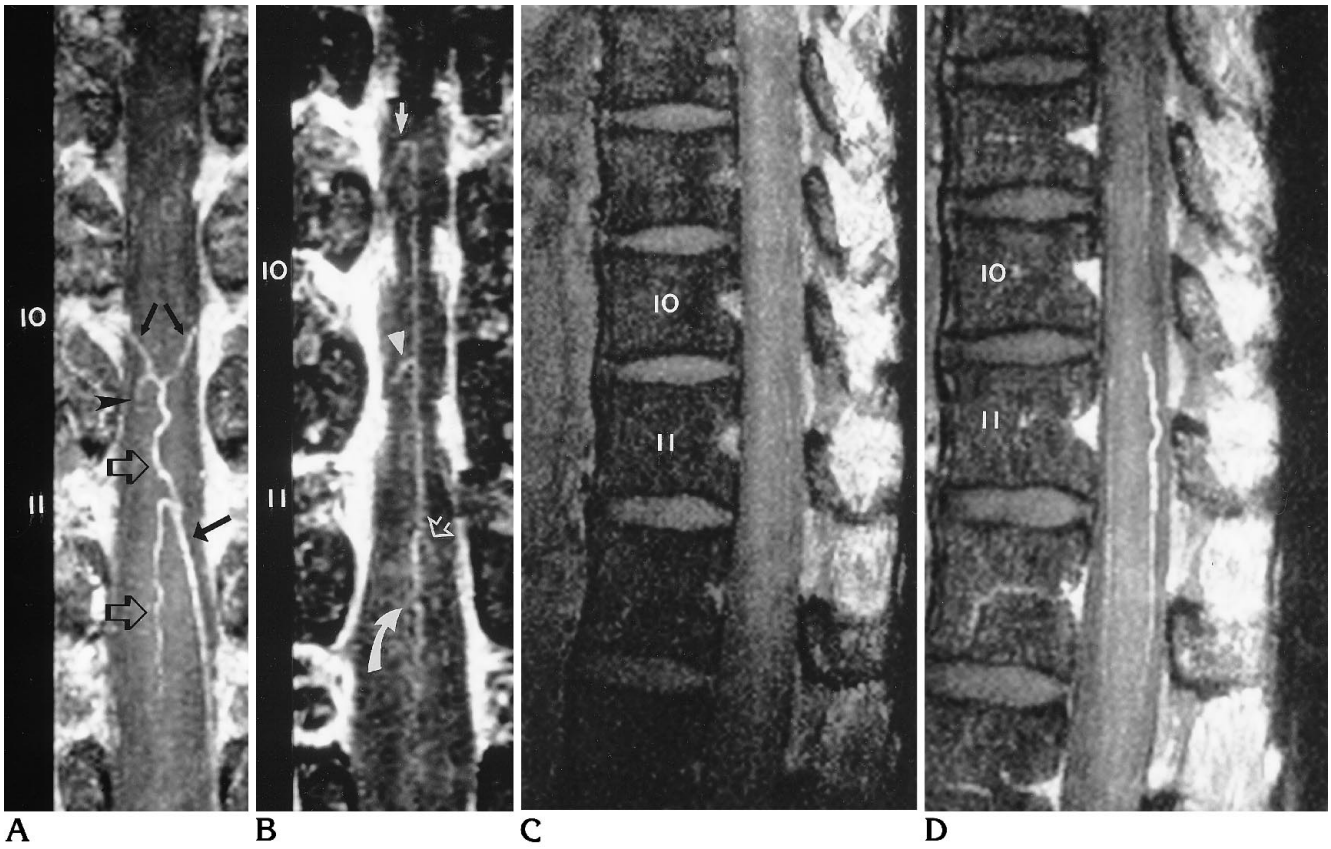

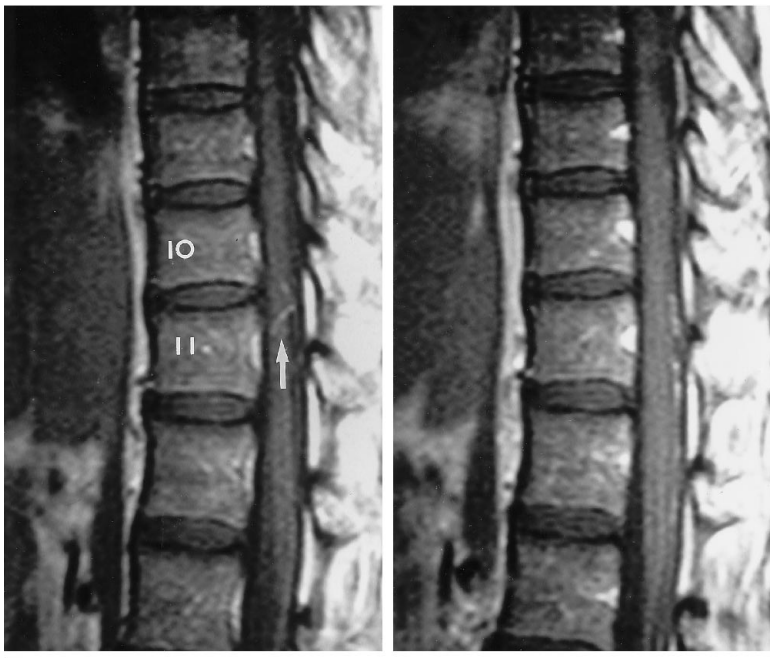

Fig 3. MR angiography and MR imaging in subject 3. Parts *A*, *B*, and *D* are produced from the same 3-D acquisition slab (sagittal orientation).

A and *B*, Postcontrast, coronal subvolume angiograms. The MIP image in *A* encompasses approximately the posterior half of the spinal canal and shows the posterior median vein (*open arrows*), the left L-1 great posterior medullary vein (*large solid arrow*), the T-10 posterior draining veins (*small solid arrows*), and the anastomotic loop at T-11 (*arrowhead*). The MIP image in *B* encompasses approximately the anterior 10% to 20% of the canal, and shows a midline vessel with features of the anterior median vein. Note the kinked segment (*curved arrow*) at T-12, corresponding to the contour seen in Figure 1D. The right T-10 anterior medullary vein (*straight arrow*) and the anastomosis (*arrowhead*) on the right side of the cord at T-11 are shown. The vessel (*open arrow*) projecting to the left of the midline and inferior to the T-11 foramen corresponds to the level of the hairpin turn of the artery of Adamkiewicz in Figure 1A. The T-10 and T-11 neural foramina are numbered.

C and *D*, Precontrast (*C*) and postcontrast (*D*) sagittal subvolume angiograms. The MIP images encompass the midline vessels and are approximately 3 mm thick. The vessels are shown well in *D* but not in *C*, and primarily correspond to the anterior and posterior median veins described above. The posterior median vein in *D* has a discontinuity at T-10, corresponding to the findings in Figures 1D and 3A.

E, Postcontrast T1-weighted right parasagittal and midsagittal images. The anastomosis (*arrow*) between the anterior and posterior median veins at T-11 is seen on the right parasagittal image. There is no enlargement or abnormal enhancement of the cord.

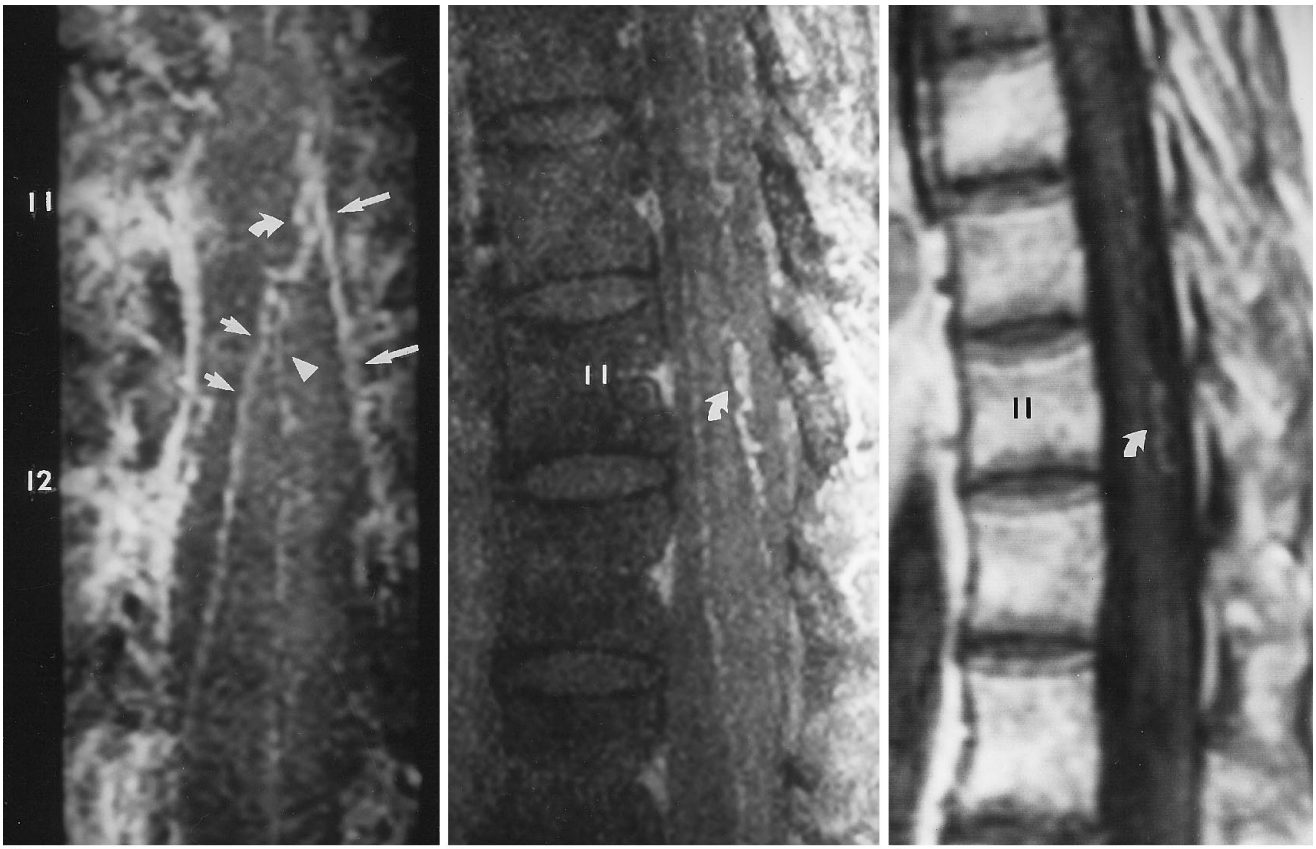

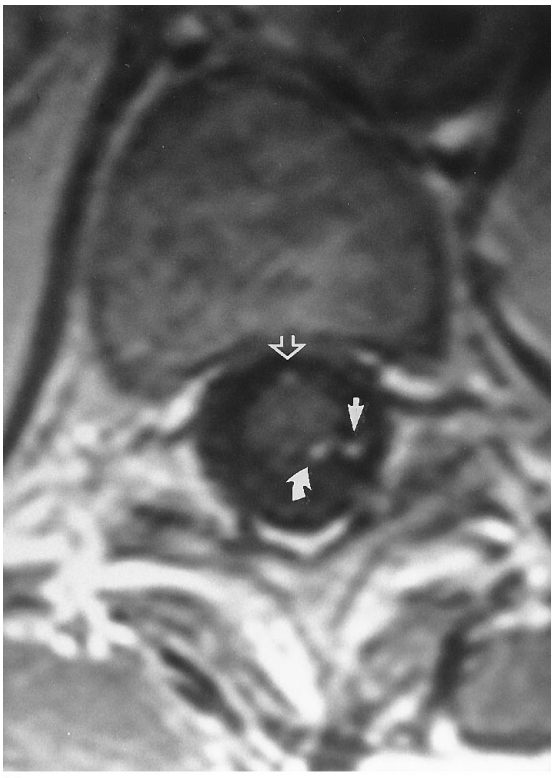

Fig 4. MR angiography and MR imaging in subject 6. Parts *A* and *B* are produced from the same 3-D acquisition slab (sagittal orientation).

A and *B*, Postcontrast coronal (*A*) and sagittal (*B*) subvolume angiograms. In *A*, the subvolume encompasses only the posterior half of the canal, and thus demonstrates the right L-1 (*short arrows*) and left T-12 (*longer arrows*) posterior medullary veins, as well as the posterior median vein (*arrowhead*) seen in Figure 2B and D. The prominent venous segment at T-11 between the origins of these veins is evident (*curved arrow*). In *B*, the subvolume MIP image (from eight source images) encompasses the midline and left paramedian portion of the cord.

C and *D*, Postcontrast sagittal (*C*) and axial (*D*) T1-weighted images at level of T-11 foramina show portions of the anterior median vein (*open arrow*), left T-12 posterior medullary vein (*solid straight arrow*), and prominent venous segment (*curved arrow*) seen in *A* and *B*. Cord size and intrinsic signal characteristics are normal.

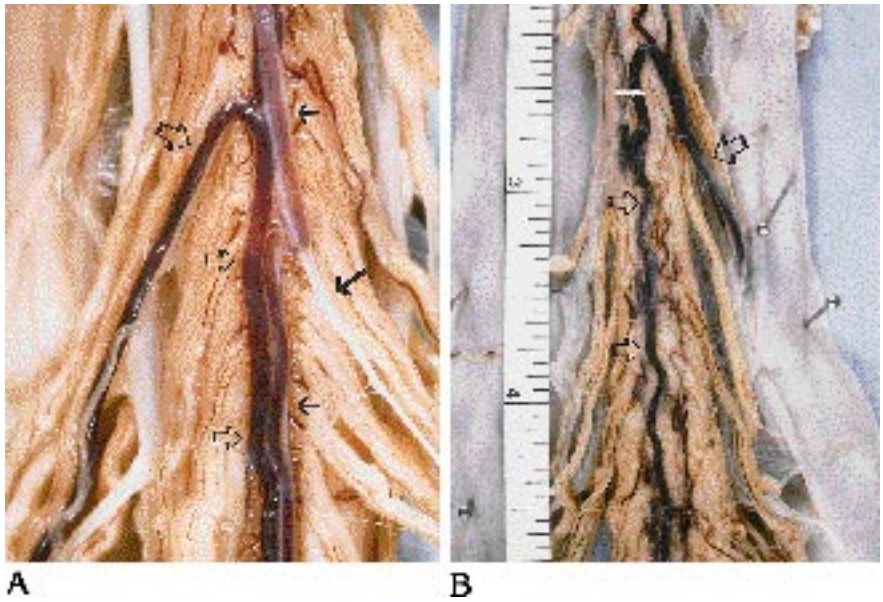

Fig 5. Postmortem spinal cord specimens *A* (*A*) and *B* (*B*). On the anterior cord surface (*A*), the anterior spinal artery (*small solid arrows*) and the artery of Adamkiewicz (*large solid arrow*) are shown. Their thicker walls distinguish them from the anterior median vein (*small open arrows*), located adjacent to the anterior spinal artery, and the great anterior medullary vein (*large open arrow*). Clotted blood is present in the veins and in the anterior spinal artery. On the posterior cord surface (*B*), there is a posterior median vein (*small open arrows*) in the midline and much smaller paramedian arteries (*solid white arrow*). Primary drainage is via the great posterior medullary vein (*large open arrow*). In comparison with the centimeter scale, the large veins are on the order of 1 mm in size. Note the coathook configuration of each medullary vein at its junction with the median vein.

lary arteries (7) may originate from the parent artery. The radicular artery, with anterior and posterior branches, supplies the corresponding nerve roots at each spinal segment (7). Radicular arteries are very small (less than 0.25 mm in diameter [5]) and are seldom shown by catheter angiography (15). These arteries are the radicular subtype of spinal "radicular" arteries in the nomenclature of Lasjaunias and Berenstein (15). The medullary artery, which supplies the cord, is not present at all segmental levels. It may exist as only a single anterior branch, measuring approximately 0.5 to 1.0 mm in diameter, or as a smaller posterior branch, at a given level (Fig 6). The medullary arteries have been termed radiculomedullary arteries by Doppman and colleagues (12). Lasjaunias and Berenstein (15) refer to the anterior medullary artery as a radiculomedullary artery and to the posterior medullary artery as a radiculopial artery, each being a subtype (total of three subtypes) of spinal "radicular" artery. There are approximately 6 to 10 (5, 7, 15), and up to 14 (14), anterior medullary arteries that contribute to the anterior spinal artery. In the thoracolumbar region, there is always a dominant, great anterior medullary artery, or artery of the lumbar enlargement, called the artery of Adamkiewicz (Figs 1A, 2A, and 5A). It originates between T-9 and T-12 in 62% (8) to 75% (15) of cases, although a frequent origin at L-1 or L-2 was noted by Gillilan (7).

The anterior spinal artery varies in size from approximately 0.2 to 0.5 mm in the cervical and thoracic regions to 0.5 to 0.8 mm in the thoracolumbar region (postmortem injected specimens [14]). The greatest diameter is at and immediately caudad to the entrance of the artery of Adamkiewicz, which usually measures from 0.5 to 0.8 mm, but may be as large as 1.0 (14) to 1.2 mm (15) in diameter. In the thoracolumbar region, the course of the anterior spinal artery varies from straight to slightly serpiginous. Caudally, it forms anastomoses with the terminal branches of the posterolateral spinal arteries. The paired posterolateral arteries, which are usually less than 0.4 mm in diameter, are dominant yet variable longitudinal channels within the pial plexus on the posterior surface of the cord (Figs 2 and 6). Posterior (paramedian) arteries may also be present, especially in the thoracic spine (14). The posterior medullary arteries, which supply the posterolateral or posterior spinal arteries, measure approximately 0.2 to 0.5 mm in the thoracolumbar region (14) and are usually difficult to see on angiograms (15), except in the vicinity of the lumbar enlargement (Fig 2C) (7). There is no longitudinal arterial trunk in the midline posteriorly (Figs 1, 2, and 5B).

Veins.—The venous drainage of the spinal cord proceeds by way of intrinsic and extrinsic veins (Fig 6). The extrinsic veins constitute the coronal venous plexus. Their courses are indepen-

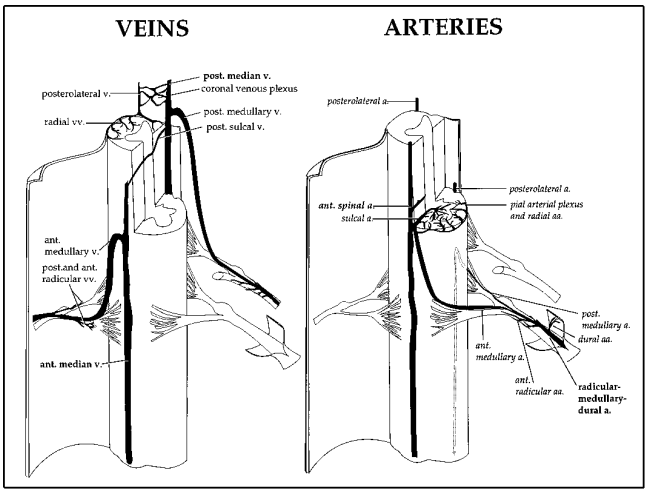

Fig 6. Schematic diagram of thoracolumbar spinal cord arterial supply and venous drainage. Anterior medullary arteries or veins accompany the anterior nerve roots, and the posterior medullary arteries or veins accompany the posterior nerve roots. The spinal cord arteries and veins each have an extrinsic or superficial system encircling the cord surface and a deeper, intrinsic system. The intrinsic vessels are usually too small to be resolved adequately on angiographic images. The extrinsic arterial system consists of the anterior spinal artery and the pial plexus with longitudinally oriented channels, including the posterolateral spinal arteries (15). The extrinsic venous system consists of the pial coronal venous plexus, which includes the median veins. The anterior median vein is located in the anterior median fissure immediately deep and to the side of the anterior spinal artery. The posterior median vein is the dominant vessel (singlet configuration) on the posterior surface of the cord in the thoracolumbar region, but may be accompanied by two comparable posterolateral longitudinal veins (triplet configuration), which lie adjacent to the posterior nerve roots, in the thoracic region (10, 11).

dent of the arteries, except for the anterior median (spinal) vein, which often parallels the anterior spinal artery (14). In the thoracolumbar spine, the anterior median vein is usually a single, midline trunk, ranging in size from 0.5 to 1.5 mm (11). The posterior median vein is distinctive, since there is no posterior midline artery (Fig 5B). The size of the posterior median vein on postmortem specimens is reported by some anatomists to be about the same (11, 14) or smaller (10) than the anterior median vein. Other investigators report that the posterior median vein is always larger (5), measuring up to 2 mm in the thoracolumbar region. Fried et al (16) found that the posterior median vein was the largest vessel on the cord surface on selective spinal angiograms, measuring 1 to 2 mm in diameter. The posterior median vein terminates in a perimedullary plexus, which communicates with the anterior median vein, and in posterior medullary vein(s), which drain to the epidural venous plexus. The posterior median vein and other posterior coronal veins tend to be more tortuous than the veins on the anterior and lateral cord surfaces, and their tortuosity increases with age (10).

The medullary veins that drain blood from the coronal plexus on the cord surface are not present at every segmental level and are not concomitant with the medullary arteries (10, 19, 20). Doppman et al and Fried et al (12, 16) refer to these veins as radiculomedullary veins. Much smaller veins, called radicular veins by Gillilan, drain the nerve roots at every segment (10). French anatomists Moes and Maillot (11) also distinguish between veins that drain the cord and those that drain the nerve roots, calling the former (ie, the medullary veins) "les veines radiculaires," and the latter (ie, the radicular veins) "les veines radicellaires." Other investigators (5, 14, 15) refer to all veins accompanying nerve roots as radicular veins.

The number of anterior medullary veins ranges from 8 to 14 (10) to approximately 20 (15), with a similar (15) or larger (10) number of posterior medullary veins. They are generally larger than the medullary arteries (14). The largest (1.5 to 2.0 mm) are in the thoracolumbar region, identified as the great anterior and/or great posterior medullary vein(s) (Fig 5). They usually accompany the corresponding anterior or posterior root between T-11 and L-3 (10, 15, 16). As indicated in the Table, medullary veins, usually the posterior ones, are routinely seen on postcontrast MR angiograms. They may be identified on postcontrast T1-weighted spin-echo images (Fig 4D) and should not be mistaken for enhancing nerve roots (21). The configuration of a medullary vein where it joins either the anterior or posterior median vein has been described as a coathook (16). The medullary vein penetrates the dura with the nerve root (22) or through a separate foramen (23) a few millimeters cephalad or caudad to the exit of the nerve root.

Technical Considerations

As has been shown for intracranial vessels (24–26), intravascular contrast material often improves the visibility of small vessels and is essential to the detection of spinal intradural vessels by means of the technique described

here (Fig 3C and D). A contrast bolus technique, such as the one we have used, provides small-vessel detail equivalent to that achieved by constant infusion during scanning (26). There are drawbacks to postcontrast MR angiography (24). One of these is the inability of flow presaturation pulses to suppress signal adequately from the contrast-containing flowing blood. In theory, this could limit the opportunity to display arteries versus veins selectively using presaturation bands; however, selective presaturation to distinguish spinal arteries from veins on time-of-flight acquisitions without contrast material is likely to be difficult at best, given the size, course, direction of flow, and hemodynamics of these vessels. For example, portions of the anterior spinal artery have bidirectional flow, and the same is likely true for the median veins, at least in the thoracic region (15). A second drawback is that contrast enhancement of a mass or of the cord itself in pathologic conditions may obscure or mimic the enhancement within spinal vessels; however, this was not a problem in the study by Bowen et al (4). Because flow enhancement at MR angiography, without or with contrast material, may be mimicked by subacute thrombus, it is prudent to obtain T1-weighted and T2-weighted spin-echo MR images, as well as MR angiographic source images before contrast material is administered. Careful evaluation of all images for thrombus should avoid this pitfall. Another potential pitfall is confusion between a normal medullary vein and nerve root enhancement (21). The medullary vein and root may be distinguished, though, if there is continuity of the vein with a vessel on the cord surface, such as the anterior or posterior median vein.

The 3-D time-of-flight technique used here does not allow de novo differentiation of the anterior median vein and anterior spinal artery. However, on the basis of having identified some contour differences between the anterior median vein and the anterior spinal artery, as well as having detected associated anterior medullary and anastomotic veins on MIP images and DSA images (Figs 1 and 3), we conclude that the anterior median vein is the anterior midline vessel primarily seen on postcontrast time-of-flight MR angiograms. Our findings do not exclude the possibility that some parts of the midline vessel on MIP images represent the anterior spinal artery alone or an unresolved combination of the anterior median vein and anterior spinal artery (Fig 3B). Why might the anterior median vein be detected instead of the anterior spinal artery? The most likely reason is that the anterior median vein is usually larger than the anterior spinal artery. Other possible explanations are (*a*) the greater pulsatility within the anterior spinal artery and (*b*) the higher velocities, which produce greater acceleration around the hairpin turns at the junctions of the anterior medullary arteries and the anterior spinal artery. Both these phenomena would contribute to phase dispersion when compared with the slower, less pulsatile flow in the medullary veins and anterior median vein. Differentiating normal intradural arteries from veins on the basis of velocities may be possible by using phase-contrast MR angiographic techniques with phase-difference data processing (27).

Normal versus Abnormal Vessels

The subjects included in this study were symptomatic and had objective evidence of myelopathy. However, each had normal findings on spinal DSA images and, except subject 4, on routine MR images of the cord. All potential segmental arterial contributions to the anterior spinal artery were investigated by means of DSA, and images were obtained into the venous phase. In the thoracolumbar region, an orderly progression of vascular opacification occurred when the catheter was not wedged. Normal intradural veins were usually seen within 15 seconds of injection, and no later than 22 seconds. In subjects 4 and 5, open biopsy was performed, and no abnormal intradural vessels were identified at the time of surgery (Table).

A relatively large, posterior paramedian venous segment was identified in subject 6 (Figs 2 and 4). This was opacified in the normal temporal sequence on DSA and drained to two sequential great posterior medullary veins. Although the paramedian segment may seem atypical, the presence of a few short, enlarged venous segments (varices) on the surface of normal cord specimens has been a common finding (11, 14). In subject 3 (Figs 1 and 3), the posterior median vein was discontinuous at T-10, draining to both neural foramina at this level via veins that followed an ascending, rather than the typical descending, course. Although an ascending course may be atypical, it has been observed elsewhere (see Fig 4 in Gilli-

lan [10]) and in our study that these veins were opacified in the normal temporal sequence. Could subjects 3 and/or 6 have had thrombosed segments of the posterior median vein, accounting for these findings? This seems unlikely, since no abnormal signal corresponding to either acute, subacute, or chronic thrombus was identified on the precontrast spin-echo or gradient-echo (MR angiography) acquisitions.

In summary, postcontrast 3-D time-of-flight MR angiography of the thoracolumbar spine in patients with normal vessels by DSA detects primarily or exclusively the largest veins on the cord surface and those extending from the cord to the epidural venous system. Anteriorly, these intradural veins are the anterior median vein and the draining anterior medullary veins. Posteriorly, these veins are the posterior median vein and the draining posterior medullary veins, especially the great posterior medullary vein. Some portions of the anterior median vessel could represent parts of the anterior spinal artery in addition to or in place of the anterior median vein, since the artery and vein are located adjacent to each other in the midline. For the posterior median vein, there is no corresponding midline artery. Thus, a dominant midline vessel on the posterior aspect of the cord on MR angiograms almost certainly represents the posterior median vein, and vessels extending from it to the dural surface represent posterior medullary veins. These medullary veins are straight, whereas the posterior median vein may have mild tortuosity over a length of a few spinal segments. In view of these normal findings, excessive tortuosity, size, and number of vessels on the posterior surface of the cord, extending over several segments and in association with a tortuous medullary vein, should suggest the possibility of enlarged intradural veins, which in the proper clinical setting may be associated with an arteriovenous malformation or dural fistula (4).

Acknowledgments

We thank John Doppman, MD, for a critical review of the preliminary manuscript. We are indebted to Kathe Holmes and Guillermo Figueredo for technical assistance, Lisa Kornse for help in monitoring the clinical histories and care of the subjects reported here, and Jean Alli and Ana Sammons for assistance in the preparation of the manuscript.

References

1. Gelbert F, Guichard J-P, Mourier KL, et al. Phase-contrast MR angiography of vascular malformations of the spinal cord at 0.5T. *J Magn Reson Imaging* 1992;2:631–636
2. Provenzale JM, Tien RD, Felsberg GJ, Hacien-Bey L. Spinal dural arteriovenous fistula: demonstration using phase contrast MRA. *J Comput Assist Tomogr* 1994;18:811–814
3. Mascalchi M, Bianchi MC, Quilici N, et al. MR angiography of spinal vascular malformations. *AJNR Am J Neuroradiol* 1995; 16:289–297
4. Bowen BC, Fraser K, Kochan JP, Pattany PM, Green BA, Quencer RM. Spinal dural arteriovenous fistulas: evaluation with magnetic resonance angiography. *AJNR Am J Neuroradiol* 1995;16:2029–2043
5. Suh TH, Alexander L. Vascular system of the human spinal cord. *Arch Neurol Psychiatry* 1939;41:659–677
6. Herren RY, Alexander L. Sulcal and intrinsic blood vessels of human spinal cord. *Arch Neurol Psychiatry* 1939;41:678–687
7. Gillilan LA. The arterial blood supply to the human spinal cord. *J Comp Neurol* 1958;110:75–103
8. Jellinger K. *Zur Orthologie und Pathologie der Ruckenmarksdurchblutung*. New York: Springer-Verlag, 1966
9. Lazorthes G, Gouaze A, Bastide G, Soutoul JH, Zadeh O, Santini JJ. La vascularisation arterielle du renflement lombaire. Etude des variations et des suppleances. *Rev Neurol* 1966;114:109–122
10. Gillilan LA. Veins of the spinal cord: anatomic details; suggested clinical applications. *Neurology* 1970;20:860–868
11. Moes P, Maillot C. The superficial veins of the human spinal cord: essay of a systemization. *Arch Anat Histol Embryol* 1981;64:5–110
12. Doppman JL, DiChiro G, Ommaya AK. *Selective Arteriography of the Spinal Cord*. St Louis: Warren H. Green, 1969:3–17
13. Djindjian R, Hurth M, Houdart R. *L'angiographie de la Moelle Epiniere*. Paris: Masson, 1970:2–75
14. Thron AK. *Vascular Anatomy of the Spinal Cord: Neuroradiological Investigations and Clinical Syndromes*. New York: Springer-Verlag; 1988;7:3–65
15. Lasjaunias P, Berenstein A. Functional vascular anatomy of the brain, spinal cord and spine. In: Lasjaunias P, Berenstein P, eds. *Surgical Neuroangiography*. New York: Springer-Verlag, 1987;3: 15–87
16. Fried LC, Doppman JL, DiChiro G. Venous phase in spinal cord angiography. *Acta Radiol* 1971;11:393–401
17. Adamkiewicz A. Die Blutgefasse des mehschilchen Ruckenmarkes. I. Die Gefasse der Ruckenmarkssubstanz. *Sitzungsb d.k. Akad. d. Wissensch in Wien. math-naturw. Cl.* 1881;84:469–502
18. Kadyi H. *Ueber die Blutgefasse des menschilichen Ruckenmarkes; nach einer im XV. Bande der Denkschriften der mathnaturw. Classe der Akademie der Wissenschaften in Krakau erschienenen Monographie, aus dem Polnischen ubersetzt vom Verfasser*. Lemberg, Poland: Gubrynowicz & Schmidt, 1889
19. Enzmann DR. Vascular diseases. In: Enzmann DR, LaPaz RL, Rubin JB, eds. *Magnetic Resonance of the Spine*. St Louis: Mosby-Year Book, 1990:510–539
20. Rosenblum B, Oldfield EH, Doppman JL, DiChiro G. Spinal arteriovenous malformations: a comparison of dural arteriovenous fistulas and intradural AVM's in 81 patients. *J Neurosurg* 1987; 67:795–802
21. Lane JI, Koeller KK, Atkinson JLD. Enhanced lumbar nerve roots in the spine without prior surgery: radiculitis or radicular veins? *AJNR Am J Neuroradiol* 1994;15:1317–1325
22. Sterzi G. Die Blutgefasse des Ruckenmarks. Untersuchungen uber ihre vergleichende Anatomie und Entwichlungsgeschichte. *Anat Hefte I Abt* 1904;24:1–364

23. Kendall HE, Logue V. Spinal epidural angiomatous malformations draining into intrathecal veins. *Neuroradiology* 1977;13:181–189
24. Chakeres DW, Schmalbrock P, Brogan M, Yuan C, Cohen L. Normal venous anatomy of the brain: demonstration with gadopentetate dimeglumine in enhanced 3-D MR angiography. *AJNR Am J Neuroradiol* 1990;11:1107–1118
25. Creasy JL, Price RR, Presbrey T, et al. Gadolinium-enhanced MR angiography. *Radiology* 1990;175:280–283
26. Sze G, Goldberg SN, Kawamura Y. Comparison of bolus and constant infusion methods of gadolinium administration in MR angiography. *AJNR Am J Neuroradiol* 1994;15:909–912
27. Bernstein MA, Ikezaki Y. Comparison of phase-difference and complex-difference processing in phase-contrast MR angiography. *J Magn Reson Imaging* 1991; 1:725–729